Biophysical Journal Volume 72 March 1997 1278–1286

Theoretical Considerations on Myofibril Stiffness

Mario Forcinito, Marcelo Epstein, and Walter Herzog
Department of Mechanical Engineering, Human Performance Laboratory, The University of Calgary, Calgary, Alberta T2N 1N4, Canada

ABSTRACT A discrete model of the interaction between individual myofilaments was developed to study the stiffness of a sarcomere for the case in which filament compliance is not negligible. Our model retains, in the limit, the characteristics of the previously published model by Ford et al. (Ford, L. E., A. F. Huxley, and R. M. Simmons. 1981. The relation between stiffness and filament overlap in stimulated frog muscle fibres. *J. Physiol.* 311:219–249). In addition, the model is able to model the interaction in cases in which few cross-bridges are attached, or when the distribution of attached cross-bridges is not uniform. Our results confirm previous indications that it might be impossible to calculate the number of attached cross-bridges by using only stiffness measurements in quick-stretch (or release) experiments.

INTRODUCTION

According to the cross-bridge theory (Huxley, 1957; Huxley and Simmons, 1971), force production in skeletal muscle occurs through formation of linkages (cross-bridges) between thick (myosin) and thin (actin) filaments. Furthermore, it is assumed that the thick and thin filaments slide rigidly past one another during contraction: that is, any compliance in the thick-filament — cross-bridge — thin-filament complex is associated with the cross-bridges. Therefore, quick release or quick stretch experiments were used to determine actomyosin stiffness, and from the stiffness values, the number of attached cross-bridges was calculated. For rigid myofilaments, the relation between stiffness and number of attached cross-bridges obtained in this way is linear (Ford et al., 1981).

Recent experimental evidence suggests that actin and myosin filaments are not perfectly rigid, but elongate when a muscle goes from a relaxed to a contracted state (Kojima et al., 1994; Huxley et al., 1994; Wakabayashi et al., 1994; Goldman and Huxley, 1994). Although these elongations are only in the order of a fraction of a percent (~0.2% for the actin filament, Kojima et al., 1994), the length of the filaments compared with the length of the cross-bridges is so large that as much as 50% of the fiber compliance has been associated with the myofilaments (Higuchi et al., 1995). Since in the past two decades many conclusions about skeletal muscle mechanics have relied on calculations of the number of attached cross-bridges based on stiffness measurements, these conclusions must be revisited with the new experimental findings in mind.

Ford et al. (1981) addressed the problem of instantaneous stiffness and its relation to the number of attached cross-bridges. They used a model consisting of linear elastic rods to represent the thick and thin filaments, and a continuous material that transfers force proportionally to the distortion, to represent the cross-bridges. Distortion in their model becomes an internal variable that can be related to the geometry of the sarcomere. Our model proves to be more general than that presented by Ford et al. (1981) and, although simplified in structure, it can be used to draw useful conclusions about the mechanical properties of sarcomeres.

It is widely accepted that, in a contracting skeletal muscle, the link between thick and thin filaments is physically realized through millions of myosin molecules attaching to specific actin sites. Because of the huge number of links, a continuous model of force transfer between representative filaments seems appropriate. However, consider the myosin filament: its total length is ~1600 nm. It has a central bare zone of ~160 nm, which leaves 720 nm for the cross-bridges on each side of the center. The separation between successive cross-bridges facing a given thin filament is ~43 nm: that is, only 17 cross-bridges can be formed between a given pair of thick and thin filaments at maximum overlap length. For less than optimal overlap, therefore, the validity of the continuum assumption may be questionable.

The purpose of this study is to develop a structural model of actomyosin interaction that allows the calculation of muscle (sarcomere) stiffness for any stiffness of the actin and myosin filaments, as well as the cross-bridges. Assuming that the entire sarcomere behaves like the composition of many individual filaments acting in parallel, we decided to base our model on a discrete description of the interaction between single thick and thin filaments.

METHODS

Let us start by analyzing the static behavior of a structure formed by elastic links, as shown in Fig. 1 *a*, which we call a "ladder" structure. In particular, we are interested in calculating the total stiffness of such a structure if the stiffness of the links is known. The ladder is one-dimensional, that is, points 0, 1, 2, . . . , $2N + 1$ can move only in the horizontal direction.

Each substructure formed by four springs arranged in a closed circuit is referred to as a "panel." For example, points 0–2–3–1–0 form a panel. Panels are numbered from 1 to N. The stiffness (in units of force per unit length) of each elastic link is denoted by $\mathbf{a}_i$, $\mathbf{b}_i$, and $\mathbf{m}_i$ for the links

Received for publication 4 March 1996 and in final form 2 December 1996.

Address reprint requests to M. Forcinito, Department of Mechanical Engineering, The University of Calgary, 2500 University Dr. NW, Calgary, Alberta T2N 1N4, Canada. Tel.: 403-220-3632; Fax: 403-282-8406; E-mail: maforcin@acs.ucalgary.ca.

0006-3495/97/03/1278/09 $2.00

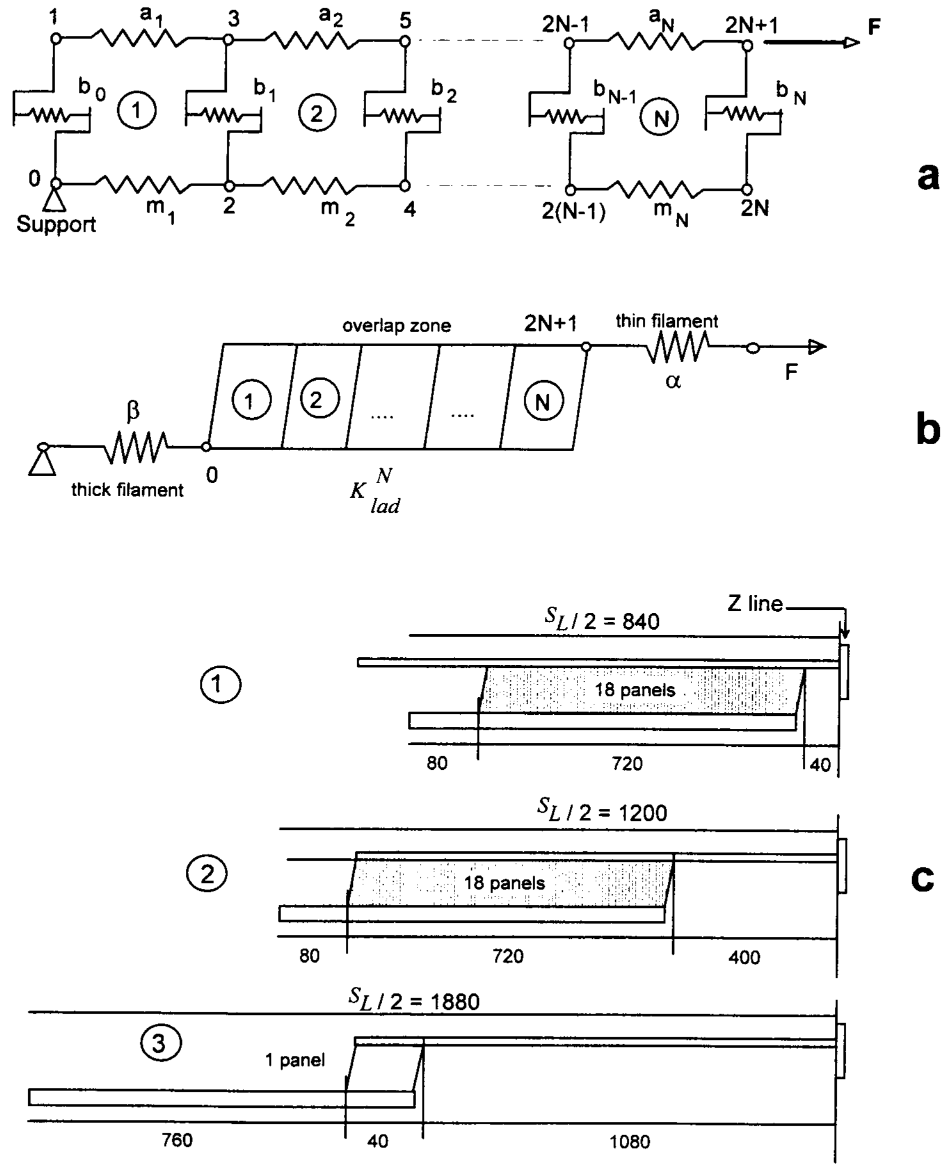

FIGURE 1 (*a*) "Ladder" structure definition. Panel numbers are circled. Joints are numbered from 0 to $2N + 1$. Joints can move in the horizontal direction only. Joint 0 is fixed. **a**, **b**, and **m** are the stiffnesses, defined as force per unit length of deformation, of the links in the actin, cross-bridges, and myosin filaments, respectively. (*b*) *N*-panel ladder structure with series elastic elements. α and β are the stiffnesses of the portion of thin and thick filaments, respectively. (*c*) Element lengths for different configurations of the ladder structure. Lengths (nm) relate the structure to the approximate sarcomere geometry of rabbit skeletal muscle.

corresponding to the actin filament, the cross-bridges, and the myosin filament, respectively.

The stiffness of a structure (measured in units of force per unit length) with $N + 1$ panels is obtained as the composition of the stiffness of the *N*-panel structure and the contribution of the three new spring elements that must be added to close a new panel. Therefore, a recursive algorithm can be used to determine the stiffness of a structure with any number of panels, starting from the solution for one panel. Details of the derivation of the algorithm are presented in Appendix A.

Ladder structure with additional series filament

The ladder structure gives a good representation of the overlap zones between filaments. However, if filament compliance is evenly distributed along the filament, sarcomere properties at lengths exceeding optimal sarcomere length may be dominated by the compliance of the filaments in the nonoverlap zone. Even a small compliance of the filaments must be taken into account in the calculation of the stiffness of the total structure.

The next step in the analysis is, therefore, to calculate the stiffness for the ladder structure with two elastic links on each side (Fig. 1 *b*). The total stiffness of the structure can be calculated by using the formula for springs in series, i.e.,

$$1/K_{\mathrm{tot}} = 1/\alpha + 1/K_{\mathrm{lad}}^{\mathrm{N}} + 1/\beta \qquad (1)$$

where K_{tot} is the stiffness of the complete structure, and $K_{\mathrm{lad}}^{\mathrm{N}}$ is the stiffness corresponding to a ladder structure having *N* panels; α and β represent the stiffness of the portions of thin and thick filaments beyond the overlap zone. Consequently, α and β are functions of the stiffness per unit length and the length of the filaments beyond the overlap zone.

To represent the approximate geometry of a vertebrate muscle sarcomere, it was assumed that each panel had a length $\delta = 40$ nm. This length was taken to approximate the repeat of the cross-bridges on the thick filament. The exact value for the cross-bridge repeat is not required for estimating sarcomere stiffness; maintaining approximate ratios of the cross-bridge repeat and the myofilament length is sufficient for adequate estimation of the sarcomere stiffness.

To simplify the calculations, it was assumed that filament lengths were similar to those of rabbit skeletal muscle and that they were integer multiples of δ. Let $L_{\mathrm{a}} = 1120$ nm, the length of the actin filament; $L_{\mathrm{m}} = 800$ nm, the length of half the thick filament; and $L_{\mathrm{o}} = 720$ nm, the length of the portion of the thick filament containing cross-bridges. The number of panels for maximum overlap is then $N_{max} = 18$. Fig. 1 *c* shows a half sarcomere for three relevant configurations.

With the dimensions defined, the sarcomere length S_L and the number of panels N_p of the ladder structure are related by:

$$\text{maximum}\{0, \text{minimum}[(L_a + L_m - S_L/2)/\delta, 18]\} = N_p \quad (2)$$

where $[x]$ denotes the integer part of x.

Parallel array of ladder structures with additional series filament

If we consider a sarcomere as an array of n filaments in parallel, the total stiffness of such a system can be calculated as:

$$K_s = \sum_{i=1}^{n} K_{tot\,i} \quad (3)$$

This formula presumes that there is no mechanical interaction between neighboring filaments, which is an approximation considering the experimental evidence reviewed in, for example, Squire (1990) and Pollack (1990).

Of course, if all ladder structures are identical, the stiffness of the array of ladders will be a multiple of the stiffness of each ladder. The array of ladder structures can be used to investigate the influence of the proportion of attached cross-bridges with respect to the total number of cross-bridges available for interaction: for each cross-bridge on each panel, the cross-bridge is attached to the thin filament if, and only if, $x_R \leq P_{att}$, where x_R is a random number in the interval [0, 1], and P_{att} is the constant probability of attachment. Remember that the analysis is done for a quasi-static case or, more properly, within an infinitesimal time period, in which it can be assumed that the structure does not change its configuration. In this case, although the overlap region for each pair of filaments has the same length, the number of panels in each unit may be different because of the random process used to generate the ladder structures. Consequently, the stiffness, K_{tot}, of each unit may also be different. Two ladder structures can have the same length but a different number of panels. In the case of missing cross-links, our model takes care of the void by combining the stiffness of the corresponding myofilament portions; therefore, panels can have different lengths, as required.

The total stiffness of the structure reflects the stiffness of the average structure, and a large number of filament pairs has the effect of reducing the dispersion of the total stiffness value with respect to the average. To calculate the average stiffness per myosin head, s, the total stiffness K_s is divided by the maximum number of cross-bridges available for interaction at the corresponding overlap and attachment proportion, $N_{CBmax} = n \cdot P_{att} \cdot (N_p + 1)$.

RESULTS

"Ladder" structure

We first consider the ladder structure with an increasing number of equal panels; this corresponds to the sarcomere overlap region gradually increasing with all the cross-bridges attached at intervals of 40 nm. Calculations of the total stiffness were performed starting from one panel with the minimum overlap possible, and going up to a hypothetical maximum of 30 panels for the case in which $\mathbf{a}_1 = \mathbf{a}_2 = \ldots = \mathbf{a}_N = \mathbf{a}$; $\mathbf{m}_1 = \mathbf{m}_2 = \ldots = \mathbf{m}_N = \mathbf{m}$, and $\mathbf{b}_0 = \mathbf{b}_1 = \ldots = \mathbf{b}_N = \mathbf{b}$, where $\mathbf{a}$ is the stiffness of a portion of the thin filament between two successive attachment sites, $\mathbf{m}$ is the stiffness of a portion of the thick filament between two myosin heads, and $\mathbf{b}$ is the stiffness of an individual cross-bridge. These conditions imply that the cross-bridges have the same elastic properties and that the distribution of attachment sites is uniform along the thin filament.

In general, the thick and thin filaments can have different elastic properties. If we write $\mathbf{a} = \rho\mathbf{m}$, a particular configuration can be defined by knowing the stiffness of a cross-bridge, $\mathbf{b}$, and the parameters $\mathbf{a/b}$ and ρ.

Intuitively, it is easy to see that for a fixed value of ρ, the total stiffness of the structure will be a linear function of the number of panels when the ratio $\mathbf{a/b}$ tends toward ∞, i.e., when the filaments become rigid. However, it is difficult to predict a priori how large the ratio $\mathbf{a/b}$ must be for the structure to behave as if the filaments were rigid.

Fig. 2 *a* shows the variations in stiffness of the ladder structure versus the ratio $\mathbf{a/b}$ for specific numbers of panels (5, 10, . . . , 30 panels) when $\rho = 1$. Experimental evidence indicates that the filaments are much stiffer than the cross-bridges, therefore attention will be given to the cases in which the stiffness of the horizontal links (filaments) is

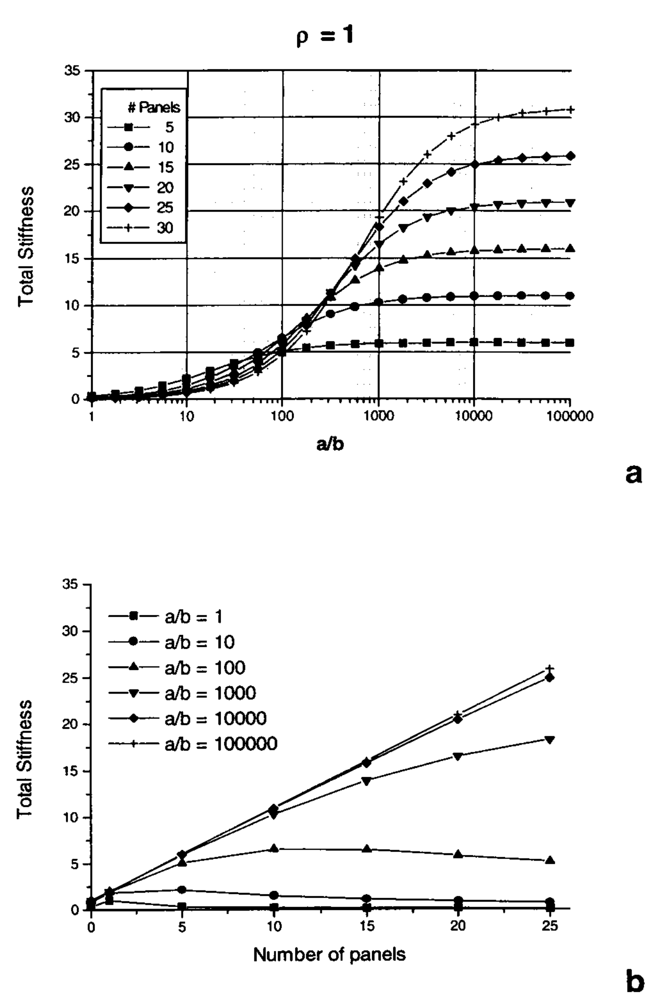

FIGURE 2 Stiffness of the ladder structure as a function of the ratio **a/b** (*top*) and the number of panels (*bottom*). The ratio **m/a** was 1 in all cases shown. The structure behaves as if the filaments were effectively rigid for **a/b** ratios of 10^5 or larger, as indicated by the flat part of the curves on the top, or the straight lines on the bottom.

much greater than the stiffness of the vertical links (cross-bridges).

Fig. 2 *b* demonstrates that the total stiffness is not a linear function of the number of panels for **a/b** $< 10^5$. This result means that even though the horizontal links (filaments) are much more rigid than the vertical links (cross-bridges), the behavior of the structure is not equivalent to that of the same structure having rigid filaments. Therefore, the proposition that the stiffness is directly proportional to the number of vertical links (i.e., attached cross-bridges) is not valid for a wide range of **a/b** ratios. Qualitatively, the behavior of the system does not change if filaments are given different stiffnesses (within the same order of magnitude), i.e., for values of ρ other than 1.

As the number of panels increases (i.e., more myofilament overlap), cross-bridges in parallel add to the total stiffness, while increasing the length of the filaments in series with the ladder structure adds to the total compliance. The total compliance of an N-panel ladder can be approximated by $1/\mathbf{b}(N+1) + N/\mathbf{a}$, which has a minimum for $N = \sqrt{\mathbf{a}/\mathbf{b}} - 1$. Note that the stiffness curves in Fig. 2 *b* have a maximum when the number of panels is $\approx \sqrt{\mathbf{a}/\mathbf{b}}$.

The conclusions extracted from the solution of the ladder structure can be applied readily to the overlap region between thin and thick filaments in one half of a sarcomere, assuming a uniform distribution of the cross-bridges.

The continuous model revisited

The discrete model presented here should be able to reproduce the limiting case in which the number of equal panels goes to infinity, while the stiffness properties are kept unaltered, (i.e., the width of the panel goes to zero). This process of going to the limit of the discrete model is one way of constructing a continuous model in which the stiffness of the filaments and the cross-bridges are given as properties per unit length. The process is described fully in Appendix B. We reproduce the result for the case in which the stiffness per unit length is the same in both filaments:

$$k_{cl} = \frac{\sigma}{(L/2 + \coth(\gamma L/2)/\gamma)} \tag{4a}$$

$$\gamma = (2\eta/\sigma)^{1/2} \tag{4b}$$

where k_{cl} is the stiffness of the overlap region, L is the overlap length, σ is the characteristic stiffness per unit length of the filaments, and η is the characteristic stiffness per unit length of the cross-bridges. Taking the term representing the overlap zone in Eq. A9 of Ford et al. (1981) for the case in which the compliances per unit length of both filaments are equal ($c_A = c_M$ following the notation therein), we obtain:

$$C_f = 1/k_{cl} = \frac{c_A}{2}\zeta + \frac{c_A}{\mu}\coth(\mu\zeta/2) \tag{5}$$

which, after applying the definitions given by Ford et al. (1981), is exactly the same as Eq. 4a.

How does Eq. 4a (or Eq. 5) compare with the results given by the discrete model? Answering this question is the same as calculating how many panels a ladder structure should have to be well-represented by the continuum approximation. Fig. 3 shows the difference between the discrete (finite number of panels) and the continuum (infinite number of panels) solutions for the overlap region between two similar filaments. Values in Fig. 3 were obtained by calculating the percent difference between the stiffness of the ladder structure, K^N_{lad}, and the stiffness calculated using Eq. 4a, k_{cl}, for the continuum structure of identical length and elastic properties. For the same number of panels, the difference is independent of the panel length and varies only slightly with the ratio between filament and cross-bridge stiffness.

Assuming that all the available myosin heads are attached simultaneously to the thin filament, only ~20 cross-bridges can be formed between a thin and a thick filament at maximum overlap (for example, in the rigor state). The number of attached cross-bridges during a tetanic contraction is likely only a fraction of those attached in rigor, implying that the continuum approach is not appropriate for representing the actin-myosin interaction (Fig. 3). Therefore, the differences in stiffness between the discrete and the continuous model cannot be neglected in cases of partial activation or in cases of small overlap between thick and thin filaments. For **a/b** ratios >1000, the term representing the stiffness of the overlap zone (second term on the left-hand side of Eq. 1) dominates; therefore, a change in the value of this second term will give about the same change in total stiffness. The dominance of this term increases for increasing stiffness of the filaments.

Although the continuum solution can be derived as a particular case of the discrete ladder structure, some of the properties of the discrete structure with a few panels are lost in the continuum solution. For a low number of panels the

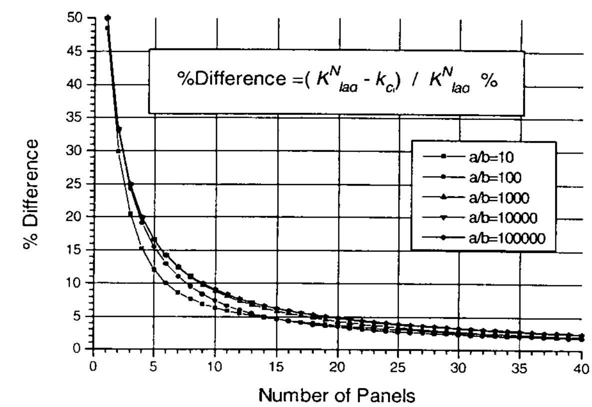

FIGURE 3 Percent difference in the stiffness between the continuum and the discrete solutions for the ladder structure. Even for 20 panels, the continuum solution gives a stiffness that is ~5% lower than the discrete solution.

continuum solution underestimates the stiffness because the implicit, continuously varied deformation gradient is different from the piecewise constant deformation gradient of each elastic link in the discrete model. In other words, the continuous model allows the transfer of forces and deformations between two consecutively attached cross-bridges, while the discrete model does not. This situation is the exact counterpart of the well-known rigidization effect of finite-difference solutions in continuous structures. Because of the discrete nature of the system under study, the discrete model is deemed as a better approximation than the continuous model.

By using the solution of the ladder structure and the sarcomere geometry given in Fig. 1 *c*, stiffness as a function of sarcomere length can be calculated using Eq. 1. The resultant stiffness of half a sarcomere is shown in Fig. 4 *a*. Clearly, as the filaments become more rigid with respect to the cross-bridges, the total stiffness approximates a direct linear relation with the number of panels (attached cross-bridges).

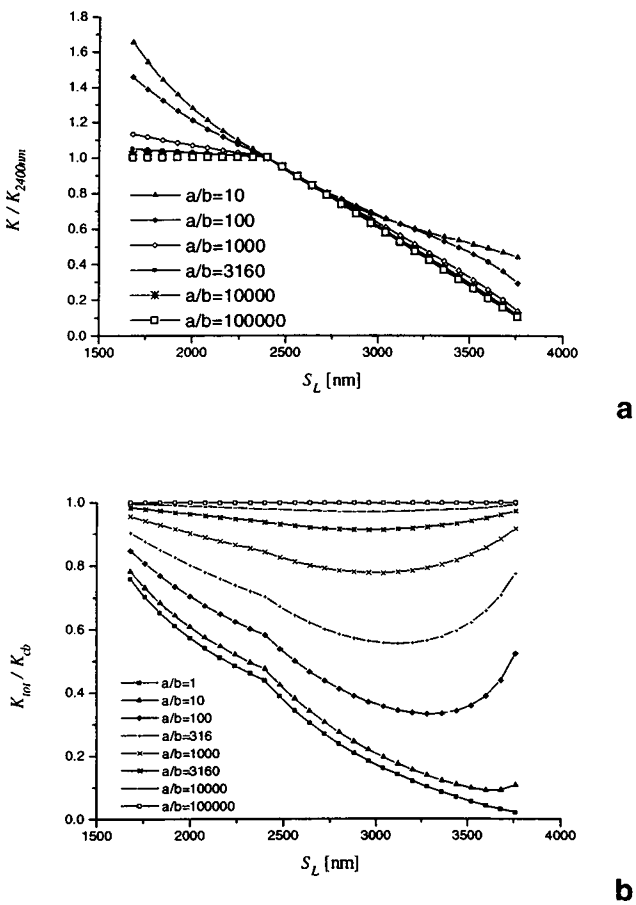

FIGURE 4 (*a*) Stiffness as a function of the sarcomere length for different stiffness ratios of the ladder structure with additional filaments. Stiffness values are plotted relative to the stiffness at 2400 nm, corresponding to configuration 2 in Fig. 1 *c*. (*b*) Ratio of total stiffness and stiffness of the overlap zone as a function of sarcomere length for different stiffness ratios. Ladder structure with additional filaments.

In Fig. 4 *a*, the stiffness was normalized with respect to the stiffness calculated at a sarcomere length of 2400 nm, the length at which myofilament overlap is maximum and no portion of the thin filament is unstressed. Fig. 4 *b* shows the ratio between the stiffness of the entire structure and the stiffness corresponding to the overlap zone as a function of sarcomere length. The graph clearly shows that the more rigid the filaments are, the closer is the stiffness of the complete structure to that of the overlap zone (ladder structure) alone.

Comparison between the present, discrete model and the continuous model of Ford et al. (1981) is shown in Fig. 5.

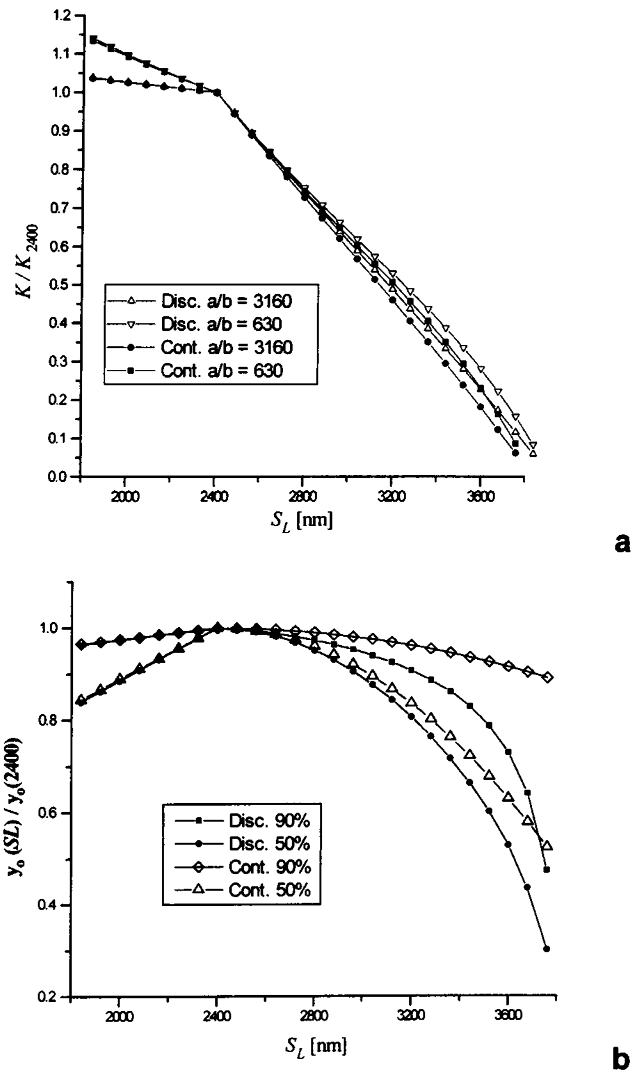

FIGURE 5 (*a*) Comparison between the stiffness given by the continuous and discrete models. Stiffness values are plotted relative to the stiffness at 2400 nm, corresponding to the optimum overlap. **a/b** = 3160 and **a/b** = 630 correspond to $\mu = 0.61\ \mu m^{-1}$ and $\mu = 1.4\ \mu m^{-1}$. (*b*) Sarcomere length dependence of y_0 plotted in the same way as Fig. 13 in Ford et al. (1981). y_0 was taken to be proportional to compliance times overlap. Comparison between discrete and continuous models: curves indicate that the longer the sarcomere the stiffer the discrete model is with respect to the continuous model with the same parameters.

Fig. 5 *a* shows the stiffness normalized relative to the stiffness at optimum overlap for both models with two biologically relevant values of the parameter **a/b**. In Fig. 5 *b*, the value of y_o, the amount of shortening that would bring the tension to zero, is normalized in the same way as Fig. 13 in the work by Ford et al. (1981). The values 90% and 50% correspond to the cases in which the cross-bridges contribute 90% and 50% of the compliance at optimum length, respectively. The difference between the continuous and the discrete model indicates that the discrete model becomes relatively stiffer than the continuous model with increasing sarcomere lengths.

Parallel array of ladder structures with additional series filament

Fig. 6 shows the total stiffness K_S and the stiffness per myosin head, *s*, calculated for a parallel array of filaments interacting in pairs. The results for a ratio **a/b** = 3160 are shown together with the corresponding results of Ford et al. (1981) for the same proportion of active cross-bridges. For a fixed overlap, variations of the stiffness per cross-bridge as functions of the proportion of attached cross-bridges are not the same for the continuous and discrete models. This result can be relevant in the study of the influence of activation.

When normalized with respect to the stiffness at a sarcomere length of 2400 nm, the total stiffness values are all nearly the same regardless of the number of filament pairs or the probabilities of cross-bridge formation. When the total stiffness is divided by the maximum number of possible cross-bridge attachments, N_{CBmax}, the measure of stiffness per cross-bridge depends on the proportion of attached cross-bridges, and is independent of the total number of filament pairs. This result implies that if the total stiffness of the system is measured, the stiffness of an individual cross-bridge cannot be calculated without measuring, in an independent way, the proportion of attached cross-bridges. This conclusion holds for both the continuous and the discrete model. However, in the discrete model, even if the proportion of attached cross-bridges is known, the number of attached cross-bridges cannot be calculated uniquely from the overall stiffness measurement, because for the discrete model the stiffness is also a function of the distribution of attachments, unlike the continuous model that was formulated for a uniform distribution of attachments. This difference between discrete and continuous models, although irrelevant in many experimental situations, could be important for in vitro assays in which very few cross-bridge links are present.

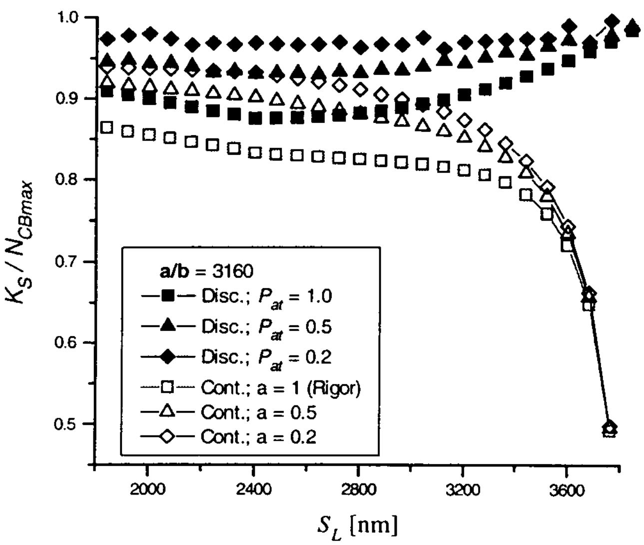

FIGURE 6 Stiffness per myosin head. Results corresponding to a parallel array of 10,000 filament pairs with additional series filament are shown with filled symbols for three different values of P_{at}, the probability of attachment of individual cross-bridges. Results corresponding to the continuous model are shown with open symbols for three different values of **a**, the proportion of attached cross-bridges. The ratio **a/b** (corresponding to rigor state) was set to 3160.

Comparison with experimental results

Higuchi et al. (1995) measured the stiffness of the thin filament to be in the range of 45–67 pN/nm for a 1-μm-long filament. Taking a value of 65 pN/nm per 1000 nm, the stiffness of a 40-nm-long portion is **a** = 1625 pN/nm. For a single cross-bridge, Nishizaka et al. (1995) reported a value for **b** ≈ 0.6 pN/nm. These numbers put the ratio **a/b** in the order of 3000; a region in which our calculations indicate that the stiffness is not linearly related to the number of attached cross-bridges.

A comparison between our numerical results and an absolute measure of stiffness, although tempting, is premature. Other factors, such as the possibility of interaction of one thick filament with several thin filaments and the effects of the distribution of attached cross-bridges on stiffness, must be addressed. A similar approach to the one presented here can be used to study a system comprised of a myosin filament interacting with six surrounding actin filaments. Also, interactions beyond those in the immediate neighborhood can be considered. If the distribution of cross-bridge attachments along the actin filament is not uniform, the problem still can be addressed using the approach presented here.

CONCLUSIONS

Based on the commonly accepted idea that interactions between actin and myosin filaments occur through cross-bridges, and the fact that only a few links can be formed between pairs of myofilaments, we developed a discrete model to calculate the stiffness of a sarcomere. The model retains the characteristic static behavior of a sarcomere.

In this study, we were only concerned with calculating the order of magnitude of sarcomere stiffness. We refrained from trying to fit numerical predictions to experimental results such as those found by Higuchi et al. (1995) and Nishizaka et al. (1995), because stiffness is very sensitive to the exact configuration of the system. Unfortunately, the exact geometry of the attached cross-bridges and their connections between the myofilaments is not completely known. If stiffness properties of actin and myosin filaments and the cross-bridges were known through in vitro experiments, a discrete model, such as the one presented here, could be used to investigate different geometries which would match the total stiffness values.

We also compared our discrete model with the continuum model developed by Ford et al. (1981). Our main conclusion was that the continuum model is not able to adequately represent a system formed by a few links. The difficulty in calculating the stiffness attributable to an individual cross-bridge without knowing the exact number of attached cross-bridges emerges, in our model, as a consequence of its sensitivity to the exact geometry of the attached cross-bridges. We have shown that it is possible to construct a model that can account for variables such as the elasticity of myofilaments and individual cross-bridges. On such a basis, and counting on the increasing sophistication in performing in vitro experiments on individual molecules, future discrete models of sarcomeres will be viable tools to help in the understanding of muscle function.

APPENDIX A

Recursive stiffness algorithm

Given the one-dimensional spring ladder shown (Fig. 1), we wish to calculate the stiffness relative to a displacement of point $2N + 1$.

We will do this inductively. Consider the case of i panels and assume that its stiffness matrix (relative to the degrees of freedom shown in Fig. A1) is known:

Therefore:

$$\mathbf{F}^{i} = \mathbf{K}^{i} \cdot \mathbf{X}^{i}$$

where the forces are given by

$$\mathbf{F}^{i} = \begin{Bmatrix} F_1^{i} \\ F_2^{i} \end{Bmatrix},$$

the displacements by:

$$\mathbf{X}^{i} = \begin{Bmatrix} X_1^{i} \\ X_2^{i} \end{Bmatrix}$$

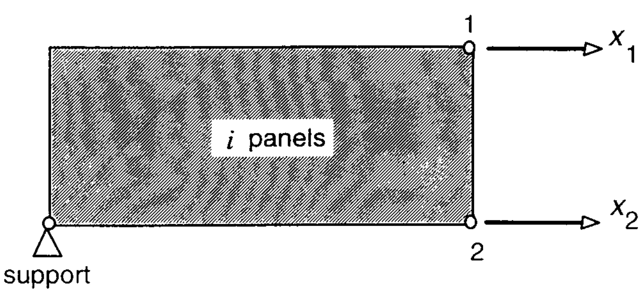

FIGURE A1 External degrees of freedom of the ladder structure with i panels.

and the stiffness matrix by:

$$[\mathbf{K}^{i}] = \begin{bmatrix} k_{11}^{i} & k_{12}^{i} \\ k_{21}^{i} & k_{22}^{i} \end{bmatrix} \tag{A1}$$

The $i + 1$-panel case will have a 4×4 stiffness matrix (with respect to the degrees of freedom shown in Fig. A2) which can be calculated as:

$$[\mathbf{K}^{i,j+1}] = \begin{bmatrix} k_{11}^{i} + a & k_{12}^{i} & -a & 0 \\ k_{21}^{i} & k_{22}^{i} + m & 0 & -m \\ -a & 0 & a + b & -b \\ 0 & -m & -b & b + m \end{bmatrix} \tag{A2}$$

Since there will be no forces applied at point 1 or 2, those degrees of freedom can be eliminated algebraically, by subdividing the 4×4 matrix into four 2×2 blocks, as follows:

$$\left[\begin{array}{cc|cc} k_{11}^{i} + a & k_{12}^{i} & -a & 0 \\ k_{21}^{i} & k_{22}^{i} + m & 0 & -m \\ \hline -a & 0 & a + b & -b \\ 0 & -m & -b & b + m \end{array}\right] \begin{Bmatrix} x_1 \\ x_2 \\ \hline x_3 \\ x_4 \end{Bmatrix} = \begin{Bmatrix} 0 \\ 0 \\ \hline F_3 \\ F_4 \end{Bmatrix} \tag{A3}$$

After the elimination is carried out, the 4×4 stiffness matrix reduces to a 2×2 matrix according to the following scheme:

$$\left[\begin{array}{c|c} \mathbf{A} & \mathbf{B} \\ \hline \mathbf{B}^{T} & \mathbf{C} \end{array}\right] \rightarrow [\mathbf{C} - \mathbf{B}^{T}\mathbf{A}^{-1}\mathbf{B}] \tag{A4}$$

4×4 2×2

In our case:

$$[\mathbf{A}^{-1}] = \frac{1}{\Delta^{i}} \begin{bmatrix} k_{22}^{i} + m & -k_{21}^{i} \\ -k_{12}^{i} & k_{11}^{i} + a \end{bmatrix} \tag{A5}$$

with:

$$\Delta^{i} = (k_{11}^{i} + a)(k_{22}^{i} + m) - (k_{12}^{i})^2 \tag{A6}$$

$$[\mathbf{B}] = [\mathbf{B}^{T}] = \begin{bmatrix} -a & 0 \\ 0 & -m \end{bmatrix} \tag{A7}$$

$$[\mathbf{C}] = \begin{bmatrix} a + b & -b \\ -b & b + m \end{bmatrix} \tag{A8}$$

Thus, the components of the stiffness matrix corresponding to $i + 1$ panels

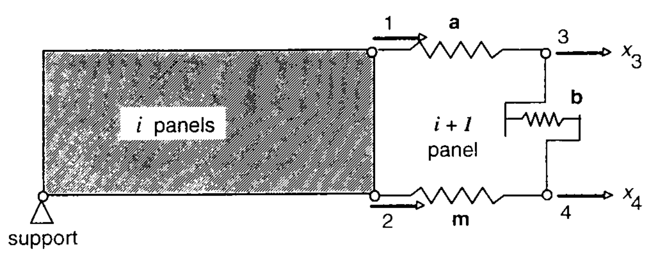

FIGURE A2 External and internal degrees of freedom when a new panel is added to the structure.

are obtained as:

$$k_{11}^{i+1} = a + b - \frac{a^2}{\Delta^i} \cdot (k_{22}^i + m) \quad \text{(A9a)}$$

$$k_{12}^{i+1} = k_{21}^{i+1} = -b + \frac{a \cdot m}{\Delta^i} \cdot k_{12}^i \quad \text{(A9b)}$$

$$k_{22}^{i+1} = b + m - \frac{m^2}{\Delta^i} \cdot (k_{11}^i + a) \quad \text{(A9c)}$$

To get a complete formulation we need an explicit expression for $[\mathbf{K}^1]$ which is obtained as:

$$[\mathbf{K}^1] = \begin{bmatrix} \frac{a \cdot b}{a + b} + b & -b \\ -b & b + m \end{bmatrix} \quad \text{(A10)}$$

Finally, once $[\mathbf{K}^n]$ has been obtained, the stiffness relative to a displacement at $2N + 1$ can again be obtained as before, because the force associated with the degree of freedom number 2 is zero:

$$K_{lad}^n = k_{11}^n - \frac{(k_{12}^n)^2}{k_{22}^n} \quad \text{(A11)}$$

APPENDIX B

The equation of Ford et al. (1981) revisited

Our departure point is the generic panel of the ladder structure, which we now recast following the notation shown in Fig. B1, where **a** and **b** are the stiffness of the filaments and cross-bridges, respectively, **h** is the panel width, and $\mathbf{u}(x)$ and $\mathbf{v}(x)$ are the displacements of the points corresponding to the lower filament and upper filament, respectively. For simplicity, we consider the case in which both filaments have the same properties.

We intend to pass to the limit as the panel width goes to zero while keeping the stiffness properties unaltered. It is clear that the stiffness of the filaments is inversely proportional to the panel width, that is, $\mathbf{a} = \sigma/\mathbf{h}$, where σ is the characteristic stiffness per unit length. The generic equilibrium equations for the upper and lower nodes are, respectively,

$$a(u_i - u_{i+1}) + a(u_i - u_{i-1}) + b(u_i - v_i) = 0 \quad \text{(B1a)}$$

$$a(v_i - v_{i+1}) + a(v_i - v_{i-1}) + b(v_i - u_i) = 0 \quad \text{(B1b)}$$

which can be recast as

$$-\frac{\sigma}{h^2}(u_{i+1} - 2u_i + u_{i-1}) + \frac{b}{h}(u_i - v_i) = 0 \quad \text{(B1c)}$$

$$-\frac{\sigma}{h^2}(v_{i+1} - 2v_i + v_{i-1}) + \frac{b}{h}(v_i - u_i) = 0. \quad \text{(B2b)}$$

Denoting $\eta = \mathbf{b/h}$, the cross-bridge stiffness per unit length, and passing to the limit as $\mathbf{h} \to 0$ while keeping σ and η constant, we obtain the ordinary differential equations:

$$-\sigma u'' + \eta(u - v) = 0 \quad \text{(B3a)}$$

$$-\sigma v'' + \eta(v - u) = 0 \quad \text{(B3b)}$$

The boundary conditions are (with the notation on Fig. B2):

$$x = 0 \rightarrow u' = 0; \quad v = 0 \quad \text{(B4a)}$$

$$x = L \rightarrow u' = 0; \quad v' = F/\sigma \quad \text{(B4b)}$$

The boundary conditions of force was obtained from a passage to the limit at the last panel.

Subtracting Eqs. B3a from B3b we obtain: $\sigma\vartheta'' = 2\eta\vartheta$ for the distortion field $\vartheta = \mathbf{u} - \mathbf{v}$ which is equivalent to Eq. [A.3] in the paper by Ford et al. (1981).

The complete solution of the system, with due account of the boundary conditions, can be expressed as:

$$u(x) = \frac{\mathbf{F}[(\mathbf{1} + e^{-\gamma L})e^{\gamma x} + (\mathbf{1} + e^{\gamma L})e^{-\gamma x}]}{\mathbf{2}\gamma\sigma(e^{\gamma L} - e^{-\gamma L})} + \frac{\mathbf{F}x}{\mathbf{2}\sigma} + \frac{\mathbf{F}(\mathbf{2} + e^{\gamma L} + e^{-\gamma L})}{\mathbf{2}\gamma\sigma(e^{\gamma L} - e^{-\gamma L})} \quad \text{(B5a)}$$

$$v(x) = -\frac{\mathbf{F}[(\mathbf{1} + e^{-\gamma L})e^{\gamma x} + (\mathbf{1} + e^{\gamma L})e^{-\gamma x}]}{\mathbf{2}\gamma\sigma(e^{\gamma L} - e^{-\gamma L})} + \frac{\mathbf{F}x}{\mathbf{2}\sigma} + \frac{\mathbf{F}(\mathbf{2} + e^{\gamma L} + e^{-\gamma L})}{\mathbf{2}\gamma\sigma(e^{\gamma L} - e^{-\gamma L})} \quad \text{(B5b)}$$

where $\gamma = (2\nu/\sigma)^{1/2}$ is identical to the quantity μ defined by Ford et al.

The stiffness of the structure can be calculated as the ratio between the force applied to the free end and the displacement of that node. Replacing

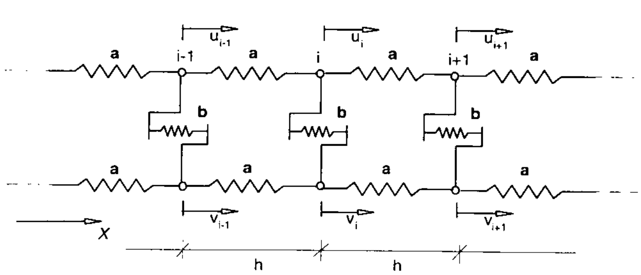

FIGURE B1 Ladder structure with infinite panels.

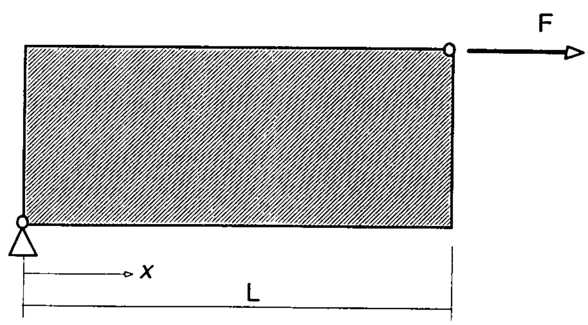

FIGURE B2 Coordinate system definition for boundary conditions.

x with L in the above expressions, the total stiffness can be expressed as:

$$k_{\mathrm{cl}} = \frac{\mathbf{F}}{\mathbf{u(L)}} = \frac{\sigma}{\mathbf{L/2} + (\mathbf{2} + e^{\gamma\mathrm{L}} + e^{-\gamma\mathrm{L}})/\gamma(e^{\gamma\mathrm{L}} - e^{-\gamma\mathrm{L}})}$$

$$= \frac{\sigma}{\mathbf{L/2} + \coth(\gamma\mathbf{L/2})/\gamma} \quad \text{(B6)}$$

We thank the reviewers for valuable comments and suggestions for improvement of the manuscript.

This work has been supported in part by a grant from the National Science and Engineering Research Council of Canada.

REFERENCES

Ford, L. E., A. F. Huxley, and R. M. Simmons. 1981. The Relation between stiffness and filament overlap in stimulated frog muscle fibres. *J. Physiol.* 311:219–249.

Goldman, Y. E., and A. F. Huxley. 1994. Actin compliance: are you pulling my chain? *Biophys. J.* 67:2131–2136.

Higuchi, H., T. Yanagida, and Y. Goldman. 1995. Compliance of thin filament in skinned fibers of rabbit skeletal muscle. *Biophys. J.* 69: 1000–1010.

Huxley, A. F. 1957. Muscle structure and theories of contraction. *Prog. Biophysics Chem.* 7:255–318.

Huxley, A. F., and R,. M. Simmons. 1971. Proposed mechanism of force generation in striated muscle. *Nature.* 233:533–538.

Huxley, H. E., A. Stewart, H. Sosa, and T. Irving. 1994. X-ray diffraction measurements of extensibility of actin and myosin filaments in contracting muscle. *Biophys. J.* 67:2411–2421.

Kojima, H., A. Ishijima, and T. Yanagida. 1994. Direct measurement of stiffness of single actin filaments with and without tropomyosin by in vitro nanomanipulation. *Proc. Natl. Acad. Sci. USA.* 91:12962–12966.

Nishizaka, T., H. Miyata, H. Yoshikawa, S. Ishiwata, and K. Kinosita. 1995. Unbinding of a single motor molecule of muscle measured using optical tweezers. *Nature.* 377:251–254.

Pollack, G. H. 1990. Muscles & Molecules, Uncovering the Principles of Biological Motion. Ebner & Sons Publishers, Seattle.

Squire, J. M., Editor. 1990. Molecular Mechanisms in Muscular Contraction. CRC Press, Inc., Boca Raton, Florida.

Wakabayashi, K., Y. Sugimoto, H. Tanaka, Y. Ueno, Y. Takezawa, and Y. Amemiya. 1994. X-ray diffraction evidence for the extensibility of actin and myosin filaments during muscle contraction. *Biophys. J.* 67: 2422–2435.